



1 **A homogenized daily *in situ* PM<sub>2.5</sub> concentration dataset from national air quality**  
2 **monitoring network in China**

3

4 Kaixu Bai<sup>1,2,3</sup>, Ke Li<sup>3</sup>, Chengbo Wu<sup>3</sup>, Ni-Bin Chang<sup>4</sup>, Jianping Guo<sup>5\*</sup>

5

6 <sup>1</sup>Key Laboratory of Geographic Information Science (Ministry of Education), East China Normal University,  
7 Shanghai, China

8 <sup>2</sup>Institute of Eco-Chongming, 20 Cuiniao Rd., Chongming, Shanghai, China

9 <sup>3</sup>School of Geographic Sciences, East China Normal University, Shanghai, China

10 <sup>4</sup>Department of Civil, Environmental, and Construction Engineering, University of Central Florida, Orlando,  
11 FL, USA

12 <sup>5</sup>State Key Laboratory of Severe Weather, Chinese Academy of Meteorological Sciences, Beijing, China

13

14

15

16 \*Correspondence to: Dr./Prof. Jianping Guo ([jpguocams@gmail.com](mailto:jpguocams@gmail.com))

17

18



19

### Abstract

20 *In situ* PM<sub>2.5</sub> concentration observations have long been used as critical data sources in haze related  
21 studies. Due to the frequently occurred haze pollution events, China started to monitor PM<sub>2.5</sub>  
22 concentration nationwide routinely from the newly established air quality monitoring network.  
23 Nevertheless, the acquisition of these invaluable air quality samples is challenging given the absence  
24 of public available data download interface. In this study, we provided a homogenized *in situ* PM<sub>2.5</sub>  
25 concentration dataset that was created using hourly PM<sub>2.5</sub> data retrieved from the China National  
26 Environmental Monitoring Center (CNEMC) via a web crawler between 2015 and 2019. Methods  
27 involving missing value reconstruction, change point detection, and bias adjustment were applied  
28 sequentially to deal with data gaps and inhomogeneities in raw PM<sub>2.5</sub> observations. After excluding  
29 records with limited temporal coverage, a homogenized PM<sub>2.5</sub> concentration dataset comprising of  
30 1,309 five-year long daily PM<sub>2.5</sub> data series was eventually compiled. This is the first thrust to  
31 homogenize *in situ* PM<sub>2.5</sub> observations in China. The trend estimations derived from the homogenized  
32 dataset indicate a spatially homogeneous decreasing tendency of PM<sub>2.5</sub> across China at a mean rate of  
33 about -7.6% per year from 2015 to 2019. In contrast to raw PM<sub>2.5</sub> observations, the homogenized data  
34 record not only has a complete data integrity but is more consistent over space and time. This  
35 homogenized daily *in situ* PM<sub>2.5</sub> concentration dataset is publicly accessible at  
36 <https://doi.pangaea.de/10.1594/PANGAEA.917557> (Bai et al., 2020a), which can be applied as a  
37 promising dataset for PM<sub>2.5</sub> related studies such as PM<sub>2.5</sub> mapping, human exposure risk assessment,  
38 and air quality management.

39 **Keywords:** PM<sub>2.5</sub>; Data homogenization; Bias correction; *In situ* observation; Air quality indicators

40

41

42

43



## 44 1 Introduction

45 A consistent  $PM_{2.5}$  concentration dataset is vital to the analysis of variations in  $PM_{2.5}$  loadings  
46 over space and time as well as in support of its risk analysis for air quality management, meteorological  
47 forecasting, and health-related exposure assessment (Lelieveld et al., 2015; Yin et al., 2020). Ground-  
48 based monitoring network is commonly built to measure concentrations of air pollutants in due course  
49 across the globe. Suffering from extensive and severe haze pollution events in the past few years (Guo  
50 et al., 2014; Ding et al., 2016; Wang et al., 2016; Cai et al., 2017; Huang et al., 2018; Luan et al., 2018;  
51 Ning et al., 2018), China launched the operational ambient air quality sampling late in 2012 on the  
52 basis of the sparsely distributed aerosol observation network. To date, this *in situ* network has been  
53 enlarged to cover almost all major cities in China consisting of about 1500 monitoring stations.  
54 Concentrations of six key air pollutants including  $PM_{2.5}$ ,  $PM_{10}$ ,  $NO_2$ ,  $SO_2$ ,  $CO$ , and  $O_3$ , are routinely  
55 measured on an hourly basis while the sampled data are released publicly online by the China National  
56 Environmental Monitoring Center (CNEMC) since 2013.

57 Although *in situ*  $PM_{2.5}$  concentration data have played critical roles in improving our  
58 understanding of regional air quality variations and relevant influential factors (Yang D. et al., 2018;  
59 Yang Q. et al., 2019; Zheng et al., 2017), little concern was raised to the quality of such dataset itself  
60 (Bai et al., 2019a, 2019c; He and Huang, 2018; Zhang et al., 2019, 2018; Zou et al., 2016). Meanwhile,  
61 few studies provided a detailed description of the accuracy or bias level (uncertainty) of the observed  
62  $PM_{2.5}$  data in recent years (You et al., 2016; Guo et al., 2017; Shen et al., 2018). The primary reason  
63 lies in the fact that neither quality assurance flag nor metadata information documenting the  
64 uncertainty other than data samplings were provided, making such quality assessment infeasible.

65 The data quality, in particular the data homogeneity, is of critical importance to the exploration  
66 of the given dataset, especially for trend analysis (Bai et al., 2019c; C. Lin et al., 2018; Liu et al., 2018;  
67 Ma et al., 2015) and data integration (Bai et al., 2019b, 2020b; T. Li et al., 2017; Zhang et al., 2019)  
68 in which a homogeneous dataset is absolutely essential for downstream applications. Since two distinct  
69 kinds of instruments are used in the current air quality monitoring network to measure near surface  
70  $PM_{2.5}$  concentration around China (Bai et al., 2020), imperfect instrumental calibration and intermittent



71 replacement of instruments may thus introduce obvious issue of discontinuity in  $PM_{2.5}$  observations.  
72 Such inhomogeneity may result in large uncertainty and even biased results in the subsequent analysis,  
73 especially in context-based and data driven  $PM_{2.5}$  concentration mapping (Bai et al., 2019b, 2019a; He  
74 and Huang, 2018; Wei et al., 2020), in which *in situ*  $PM_{2.5}$  concentration observations are used as the  
75 ground truth to characterize complex relationships with other possible contributing factors.

76 Given the absence of an open access and quality assured *in situ*  $PM_{2.5}$  concentration dataset in  
77 China, in this study, we attempted to generate a long-term coherent *in situ*  $PM_{2.5}$  concentration dataset  
78 for scientific community to use in future applications. A set of methods involving missing value  
79 reconstruction, change point detect, and bias adjustment were geared up seamlessly in a big data  
80 analytic manner to improve the data integrity and to remove discontinuities present in raw  $PM_{2.5}$   
81 observations. Such an analytical process is also referred to as data homogenization in data science or  
82 big data analytics (Cao and Yan, 2012; Wang et al., 2007). To our knowledge, this is the first thrust to  
83 homogenize a large-scale dataset of *in situ*  $PM_{2.5}$  concentration observations in China. In the following  
84 sections, we will introduce the data source as well as detailed big data analytics methods used for the  
85 creation of a homogenized  $PM_{2.5}$  concentration dataset.

## 86 **2 *In situ* $PM_{2.5}$ concentration observations**

87 In this study, the hourly  $PM_{2.5}$  concentration data sampled at more than 1,600 state-controlled air  
88 quality monitoring stations across China from January 1, 2015 to December 31, 2019 were utilized.  
89 The  $PM_{2.5}$  concentration data are routinely measured on an hourly basis using instruments such as  
90 beta-attenuation monitors and Tapered Element Oscillating Microbalance (TEOM) analyzer. The  
91 ordinary instrumental calibration and quality control are performed according to the national ambient  
92 air quality standard of GB3095-2012 and HJ 618–2011 (Guo et al., 2009, 2017). Generally, TEOM  
93 can measure  $PM_{2.5}$  concentration within the range of 0–5,000  $\mu\text{g m}^{-3}$  at a resolution of 0.1  $\mu\text{g m}^{-3}$ , with  
94 precisions of  $\pm 0.5 \mu\text{g m}^{-3}$  for 24-h average and  $\pm 1.5 \mu\text{g m}^{-3}$  for hourly average (Guo et al., 2017; Xin  
95 et al., 2012). All  $PM_{2.5}$  measurements are publicly released online by the National Urban Air Quality  
96 Real-time Publishing Platform (<http://106.37.208.233:20035/>) under the China National  
97 Environmental Monitoring Center (CNEMC) within one hour after the direct sampling.



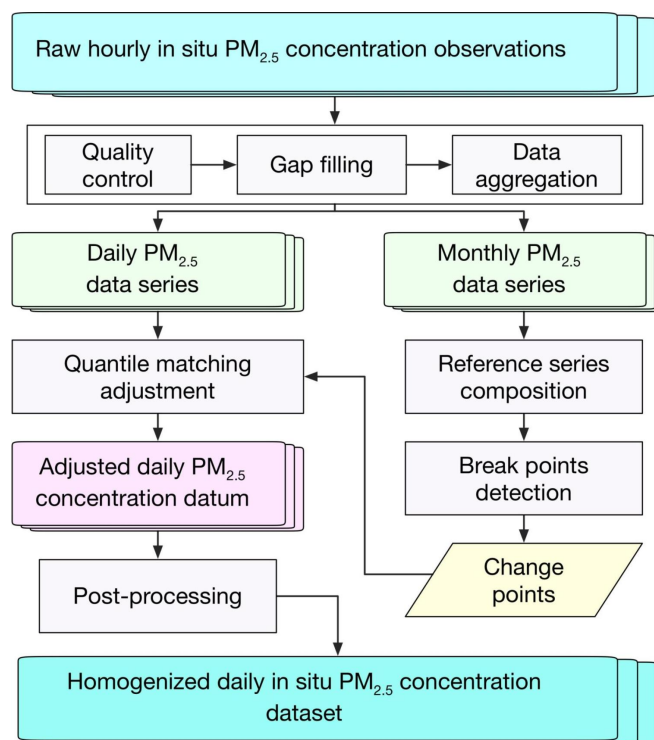
98           Although these data sampling are publicly released, the acquisition of these valuable samplings  
99           always exhibits a big challenge because no data download interface is provided to the public by the  
100          CNEMC website. Therefore, it is impossible for users to retrieve the historical observations from the  
101          given website. Rather, science community has to count on other measures such as an automatic web  
102          crawler for the retrieval of these online updated data samples from the data publishing platform.  
103          Nevertheless, the archived data records through such an approach suffered from significant data losses  
104          due to various unexpected reasons like power outage and internet interruption. Consequently, the data  
105          integrity becomes problematic and further treatments like gap filling are thus essential to accounting  
106          for such defects at least.

107          Moreover, hourly  $PM_{2.5}$  concentration observations that were sampled at five embassies of United  
108          States in China from January 2015 to June 2017 were used as an independent dataset to evaluate the  
109          fidelity of the homogenized  $PM_{2.5}$  concentration dataset. Geographic locations of these five embassies  
110          have been shown in Table S1. These  $PM_{2.5}$  data were measured independently under the U.S.  
111          department of state air quality monitoring program and can be acquired from the  
112          <http://www.stateair.net/>. To be in line with the homogenized dataset, the hourly  $PM_{2.5}$  concentration  
113          data were aggregated to the daily level by averaging the 24-h observations sampled on each date while  
114          daily averages were calculated only for days with more than 12 valid samples of a possible 24-h.

### 115   **3 Homogenization of *in situ* $PM_{2.5}$ concentration data**

116          For the creation of a long-term coherent *in situ*  $PM_{2.5}$  concentration dataset, it is necessary to  
117          create an analytical framework of the big data analytics which seamlessly gears up several methods as  
118          a whole for the purposes of gap filling, change point detection, and discontinuity adjustment. Figure 1  
119          shows a schematic illustration of the general workflow toward generating a homogenized dataset. The  
120          whole process can be outlined as follows.

- 121       (1) It is necessary to perform the essential quality control and gap filling on the raw  $PM_{2.5}$  observations  
122           so that the bias arising from large outliers and resampling errors due to incomplete observations  
123           can be reduced.



124  
125 **Figure 1.** A schematic flowchart for the creation of a homogenized daily *in situ* PM<sub>2.5</sub> concentration  
126 dataset.

- 127
- 128 (2) Short-term time series due to sites relocation were temporally merged to attain a long-term record.
- 129 Then, PM<sub>2.5</sub> concentration time series with a temporal coverage of less than four-year during the
- 130 study period were excluded and the quality-controlled observations of hourly *in situ* PM<sub>2.5</sub>
- 131 concentration were resampled to daily and monthly scales to initiate the homogeneity test.
- 132 (3) Reference time series were constructed for each long-term PM<sub>2.5</sub> concentration record using data
- 133 measured at adjacent monitoring sites in the surroundings. For PM<sub>2.5</sub> concentration records failing
- 134 to produce a reference series, no homogeneity test was performed for such datum due to the
- 135 absence of reference series.
- 136 (4) The discontinuity identified in each daily long-term PM<sub>2.5</sub> concentration time series were adjusted
- 137 using the quantile-matching (QM) adjustment method according to the detected change points in
- 138 the monthly record with the support of reference series.



139 (5) Post-processing measures such as nonpositive value correction and another round gap filling were  
140 further performed on the homogenized records to improve the quality to attain a quality-assured *in*  
141 *situ* PM<sub>2.5</sub> concentration dataset. More details of each method are described in the following  
142 subsections.

### 143 3.1 Quality control

144 Given the possibility of the presence of abnormal samplings, it is essential to removing the outliers  
145 detected in the original PM<sub>2.5</sub> observations to reduce the false alarm rate in change point detection  
146 during the subsequent homogeneity test. Specifically, hourly PM<sub>2.5</sub> concentration data values meeting  
147 one of the following criteria were excluded: 1) out of the range between 1 and 1,000  $\mu\text{g m}^{-3}$ , and 2)  
148 more than three standard deviations from the median of observations within a 15-h time window. Both  
149 criteria aimed to remove large outliers which could result in biased daily averages. Overall, 3.46% of  
150 PM<sub>2.5</sub> samples were treated as outliers which were then excluded accordingly (filled with Nan to  
151 indicate missing values).

### 152 3.2 Gap filling and resampling

153 As indicated in a recent study (Bai et al., 2020), missing value related data voids become a big  
154 obstacle in the raw PM<sub>2.5</sub> observations that were retrieved from the CNEMC website as PM<sub>2.5</sub>  
155 observations on 40% of sampling days suffered from data losses due to unexpected reasons. To reduce  
156 the impact of missing value related resampling (from hourly to daily) bias on the subsequent  
157 homogeneity test, we filled those missing value related data gaps that were found in each 24-h PM<sub>2.5</sub>  
158 observation by applying the DCCEOF method developed very recently (Bai et al., 2020b). Such a gap  
159 filling effort enabled us to improve the percentage of days without missingness during the study time  
160 period from 58.8% to 97.3%.

161 In spite of the improvement of data integrity after gap filling, the resultant PM<sub>2.5</sub> time series  
162 remain temporally discrete due to the emergence of several long-lasting (e.g., more than 24 consecutive  
163 hours) data missing episodes. Also, the hourly time series are still too noisy to be handled by the  
164 available homogeneity test software due to the significant variability of PM<sub>2.5</sub> over space and time. In  
165 such context, the hourly PM<sub>2.5</sub> concentration records were resampled to daily and monthly scales to



166 initiate the homogeneity test. Moreover, the monthly series was primarily used to detect the possible  
167 change points while the daily series was adjusted in reference to the corresponding reference series  
168 based on the change points detected from the monthly series. To avoid large resampling bias, monthly  
169 averages were calculated only for those with at least 20 valid daily means of a possible month at each  
170 site. The frequency of missing values in each month was also calculated as a possible metadata  
171 information to further examine the detected change points.

### 172 **3.3 Homogeneity test**

173 A commonly used homogeneity test software, the RHtestsV4 package, was hereby applied to  
174 detect the possible discontinuities in raw PM<sub>2.5</sub> data series that were retrieved from the CNEMC  
175 website. As suggested in Wang and Feng (2013), RHtestsV4 is capable of detecting and adjusting  
176 change points in a data series with first-order autoregressive errors. Given the low false alarm rate via  
177 change point detection and the capability to adjust discontinuity, the RHtests software packages have  
178 been widely used to homogenize climate data records such as temperature (Cao et al., 2013; Xu et al.,  
179 2013; Zhao et al., 2014), precipitation (Wang et al., 2010a; Nie et al., 2019), and other datum like  
180 boundary layer height (Wang and Wang, 2016). Two typical methods, namely the PMTred and  
181 PMFred, were embedded in a recursive testing algorithm in RHtestsV4, with the former relying on the  
182 penalized maximal *t* test (PMT) while the latter based on the penalized maximal *F* test (PMF) ( Wang  
183 et al., 2007; Wang, 2008a). With the incorporation of these empirical penalty functions (Wang, 2008a,  
184 b), the problem of uneven distribution of false alarm rate is largely alleviated with the aid of RHtestsV4.  
185 In contrast to the PMF which works without a reference series, the PMT uses a reference series to  
186 detect change points and the results are thus far more reliable (Wang, 2008a, b). The way to generate  
187 reference series will be described in the next subsection. Also, the RHtestsV4 is capable of making  
188 essential adjustments to the detected discontinuities by taking advantage of the QM adjustment method  
189 (Wang and Feng, 2013).

190 Here the PMT method rather than the PMF was used to detect change points given the higher  
191 confidence of the former method in change point detection due to the involvement of reference series  
192 (Wang and Feng, 2013). To ensure the reliability of detected discontinuities, change point was defined



193 and confirmed at a nominal 99% confidence level, and the data records were then declared to be  
194 homogeneous once no change point was identified. Subsequently, the QM adjustment method was  
195 applied to correct PM<sub>2.5</sub> observations with evident drifts with the support of reference series, namely,  
196 to homogenize PM<sub>2.5</sub> concentration data series. To avoid large sampling uncertainty in the estimate of  
197 QM adjustments, the  $Mq$  (i.e., the number of categories on which the empirical cumulative distribution  
198 function is estimated) was automatically determined by the software to ensure adequate samples for  
199 the estimation of mean difference and probability density function. Meanwhile, the number to  
200 determine the base segment (i.e.,  $Iadj$ ) was set to 0 so that datum in other segments were all adjusted  
201 to the segment with the longest temporal coverage.

### 202 3.3.1 Construction of reference series

203 A good reference series is vital to the relative homogeneity test because it helps pinpoint possible  
204 discontinuities in each base series (the data series to be tested) as well as determine the performance  
205 of the subsequent data adjustment. In general, reference series can be organized by using one specific  
206 record either measured at the adjacent station or aggregated from multiple adjacent observations (Cao  
207 and Yan, 2012; Peterson and Easterling, 1994; Xu et al., 2013; Wang et al., 2016). The most  
208 straightforward method is to use the neighboring data series either measured at the nearest station or  
209 series that are highly correlated with the base series (Peterson and Easterling, 1994; Cao and Yan,  
210 2012; Wang and Feng, 2013). Such methods, however, fail to take the repetitiveness of the neighboring  
211 series into account since the neighboring series may also suffer from discontinuities.

212 To avoid the misuse of inhomogeneous PM<sub>2.5</sub> concentration records in constructing reference  
213 series, a complex yet robust data integration scheme was developed to screen, organize, and construct  
214 reference series for each *in situ* PM<sub>2.5</sub> concentration data series. For each daily PM<sub>2.5</sub> concentration  
215 data series, all the neighboring series were firstly identified from its surroundings with a lag distance  
216 as large as of 50 km. No reference series was constructed once there was no neighboring series  
217 available within the given radius and in turn the homogeneity of the given record was not examined.  
218 Otherwise, both correlation coefficient (R) and coefficient of variation (CV) were calculated between  
219 the given base series and each selected neighboring series to assess their representativeness (Shi et al.,



220 2018; Rodriguez et al., 2019). Then, neighboring series with  $R > 0.8$  and  $CV < 0.2$  were selected as  
221 candidates to construct the reference series for a given base series.

222 The reference series was then constructed by averaging both the base and the candidate series at  
223 each observation time if there was only one candidate series. For the situation with more than one  
224 candidate series, the empirical orthogonal function (EOF) analysis was applied to these multiple  
225 candidates and then the original fields were reconstructed with the leading principal components when  
226 the accumulated variance explained by them exceeded 80%. This was expected to reduce the possible  
227 impacts of abnormal observations and short-term discontinuities in the neighboring candidates on the  
228 resultant reference series. Subsequently, the reference series were organized and constructed through  
229 a spatial weighting scheme as each reconstructed record was assigned a spatially resolved weight  
230 according to their relative distances to the base series over space. Here we applied a Gaussian kernel  
231 function to estimate the weight of one neighboring observation on the other in space and such a scheme  
232 has been proven to be effective in assessing the spatial autocorrelation of  $PM_{2.5}$  concentration (Bai et  
233 al., 2019b). Mathematically, the reference series can be constructed from the following equations:

$$234 \quad PM_{ref} = \sum_{i=1}^N \frac{w_i * PM_{cand}^i}{\sum w_i} \quad (1)$$

$$235 \quad w = \exp\left(\frac{-d^2}{2h^2}\right) \quad (2)$$

236 where  $PM_{ref}$  and  $PM_{cand}$  denote the reference and candidate series, respectively.  $N$  is the total  
237 number of candidate series while  $w$  is the spatial weight assigned to each candidate series and  $d$  is  
238 the spatial lag distance between the base and the corresponding candidate series.  $h$  is a spatial  
239 correlation length that is used to modulate the relative influence of a distant observation on the data  
240 measured at the base site. In this study, an empirical value of 50 km was assigned according to the  
241 estimated semi-variogram results (Bai et al., 2019b).

242 For any record having neighboring series within 50 km but poorly correlated ( $R < 0.8$  or  $CV > 0.2$ )  
243 to all its neighbors (meaning the base series differ from the neighbors), the reference series were  
244 created by following the same procedures as those detailed above by taking the nearest neighbor as the  
245 base series. For the situation with only one candidate series available, it is logical to compare both the  
246 base and the candidate series against another data to check which one should be corrected. It was noted



247 that the  $PM_{2.5}$  time series estimated from the MERRA-2 aerosol reanalysis in the same way as  
248 described in He et al. (2019) was used. The one more correlated to this external  $PM_{2.5}$  time series was  
249 then used as the reference (deemed as homogeneous) while the other was considered as the base series  
250 (i.e., implies to be adjusted). Such an inclusive scheme empowered us to screen and construct reference  
251 series for 1,262 long-term  $PM_{2.5}$  concentration records across the board. In contrast, no reference series  
252 were constructed for 47 isolated records.

### 253 3.3.2 Post-processing measures

254 Several post-processing measures were applied to the adjusted data records to further improve  
255 the quality of this dataset. Since nonpositive values may appear in the QM adjusted data series if the  
256 original values are close to zero (Wang et al., 2010b), nonpositive values were replaced with the  
257 smallest valid  $PM_{2.5}$  concentration amount measured at each monitoring site during the study period.  
258 Subsequently, the data gaps in the adjusted datum due to long-lasting missingness were filled by first  
259 calibrating the corresponding data values in the reference series measured on the same date (if available)  
260 to the homogenized datum level. The modified quantile-quantile adjustment (MQQA) method  
261 proposed in Bai et al. (2016) was hereby used given its adaptive data adjustment principle. For the  
262 predicted values, such MQQA scheme rendered higher accuracy than those interpolated from data  
263 values measured on adjacent dates because  $PM_{2.5}$  concentration is spatially more correlated than in the  
264 temporal domain (Bai et al., 2019b). For the remaining data gaps, those missing values were  
265 reconstructed in a similar procedure as the DCCEOF method (Bai et al., 2020b). Note that the matrix  
266 used for EOF analysis in the context of DCCEOF was constructed using the neighboring data series  
267 measured within a radius of 100 km with a temporal lag of 30 days at most. Finally, all data values  
268 were rounded to integer to be in line with the original  $PM_{2.5}$  concentration observations.

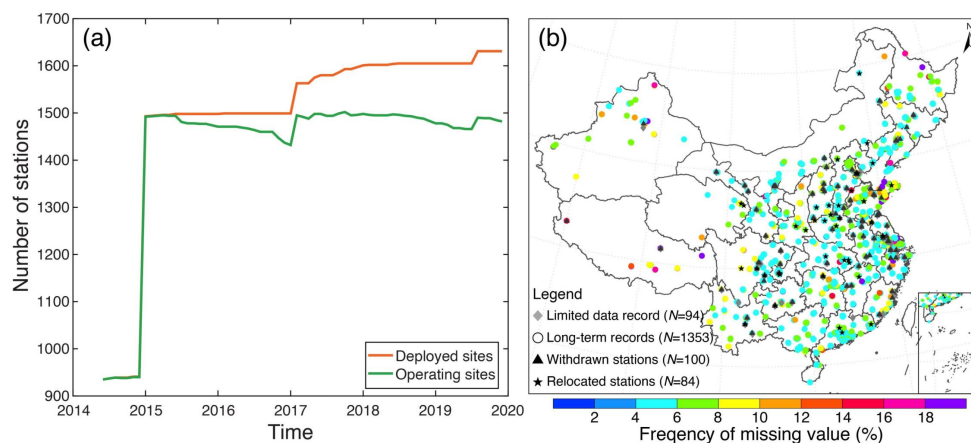
## 269 4 Results and discussion

### 270 4.1 Descriptive statistics

271 Prior to data homogenization, we first need to exclude those short-term and less reliable records.  
272 Figure 2 shows the temporal variations of the number of air quality monitoring stations deployed in  
273 China during 2015–2019 as well as the spatial patterns of the frequency of missing values for each



274 long-term  $\text{PM}_{2.5}$  concentration record. It shows that a total of about 1,630 air quality monitoring  
275 stations had been deployed in China before 2020. Nevertheless, about 1,500 sites routinely providing  
276  $\text{PM}_{2.5}$  observations were kept up in operation since 2015 (Figure 2a). By referring to the data continuity  
277 of  $\text{PM}_{2.5}$  observations, it is noticeable that 100 monitoring stations had been withdrawn before 2020  
278 because no  $\text{PM}_{2.5}$  observations were provided for more than three consecutive months since the release  
279 of their last valid data (Figure 2b). Meanwhile, 42 pairs of stations were found to be relocated since  
280 new stations at nearby started to provide  $\text{PM}_{2.5}$  observations soon after the suspension of the original  
281 site. This is also corroborated by the temporal lags of  $\text{PM}_{2.5}$  observations between original and newly  
282 deployed stations as many of them were found to have a time lag less than 15-day. Also, 94 sites were  
283 found with limited data records due to short temporal coverage (newly deployed). Finally, 1,353 long-  
284 term  $\text{PM}_{2.5}$  concentration records were identified with their first valid data released even earlier than  
285 2015. In regard to the frequency of missing value, it is indicative that data gaps were obvious in these  
286 long-term  $\text{PM}_{2.5}$  concentration records, with about 6% of hourly data values missed on ~47% of  
287 sampling days on average. This also motivates us to fill such data gaps to improve the data integrity.



288  
289 **Figure 2.** Spatial and temporal patterns of air quality monitoring stations in China. (a) Temporal  
290 variations of the total number of air quality monitoring stations in China. (b) Spatial patterns of the  
291 frequency of missing value in each long-term hourly  $\text{PM}_{2.5}$  concentration record measured from  
292 January 1, 2015 to December 31, 2019. Stations were categorized into distinct groups according to  
293 their data length and temporal continuity. The frequency of missingness was calculated as the ratio of

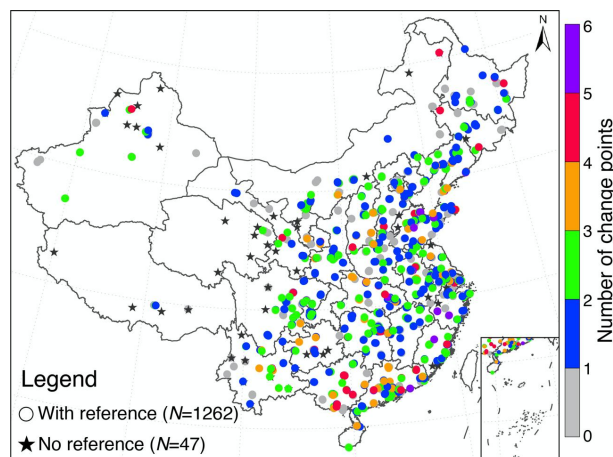


294 the number of missing values in each PM<sub>2.5</sub> concentration record to the total number of samplings from  
295 the time of the release of the first valid data to December 31, 2019.

#### 296 4.2 Homogenization of *in situ* PM<sub>2.5</sub> data

297 A total of 1,395 long-term (with five-year observations) PM<sub>2.5</sub> concentration records were  
298 acquired with the inclusion of 42 temporally merged data series at those relocated stations. After  
299 removing those suffering from more than three consecutive months data losses, 1,309 long-term yet  
300 consecutive PM<sub>2.5</sub> concentration records were obtained. The homogeneity test was finally performed  
301 on 1,262 records due to the availability of reference series. Figure 3 shows the spatial patterns of the  
302 total number of change points detected in 1,262 monthly PM<sub>2.5</sub> concentration records. The ubiquitous  
303 change points imply that there is an obvious inhomogeneity in this *in situ* PM<sub>2.5</sub> concentration dataset.  
304 About 57% (719 out of 1,262) of records failed to pass the homogeneity test due to the presence of  
305 change points. Given the overall good agreement between the base and reference series (refer to Figure  
306 S1 for the correlation coefficient and root mean square error between them), it indicated that these PM<sub>2.5</sub>  
307 concentration records did suffer from evident discontinuities. Meanwhile, the vast majority (~80%) of  
308 the inhomogeneous PM<sub>2.5</sub> records suffered from no more than two change points (Figure 3), suggesting  
309 the mean shift could be the primary reason for the detected discontinuities. Moreover, 20 records were  
310 even found suffering from no less than five significant change points, indicating phenomenal  
311 discontinuities in these records.

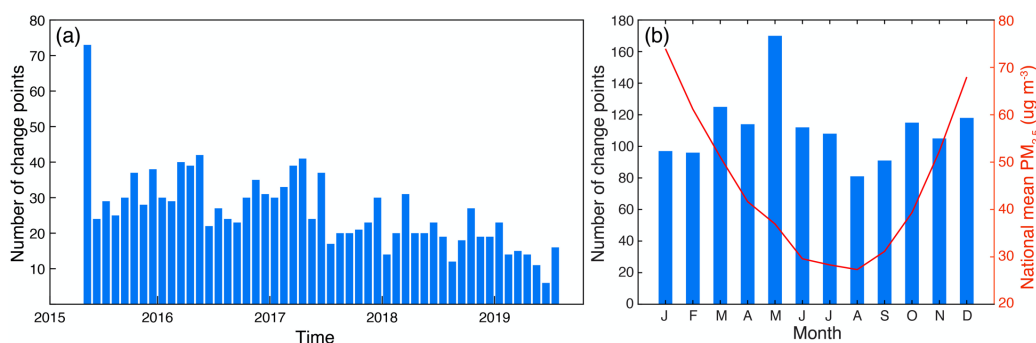
312





313 **Figure 3.** Spatial patterns of the total number of change points detected in each long-term yet  
314 consecutive PM<sub>2.5</sub> concentration records. Gray dot indicates there was no change point detected in this  
315 PM<sub>2.5</sub> concentration record.

316 Figure 4 shows the temporal variability of the number of change points detected in monthly PM<sub>2.5</sub>  
317 concentration records. As indicated, change points were detected in every specific month of the year  
318 from May 2015 to July 2019, especially in late spring (e.g., May), in which change points were more  
319 likely to be detected (Figure 4b). This is attributable to the seasonality of PM<sub>2.5</sub> loading in China as  
320 high PM<sub>2.5</sub> concentrations are always observed in the winter whereas low values in the summer.  
321 Consequently, change points were detected with larger chance during the chronic transition periods  
322 (e.g., spring to summer). In addition, it is noteworthy that a large volume of change points was detected  
323 in early 2015, indicating the existence of phenomenal discontinuities during this period (Figure 4a).  
324 After checking the temporal variations of PM<sub>2.5</sub> concentration, findings indicate that PM<sub>2.5</sub>  
325 observations varied with large deviations among each other during this period. This could be linked to  
326 the imperfect instrument calibration or irregular operation in the early stage.

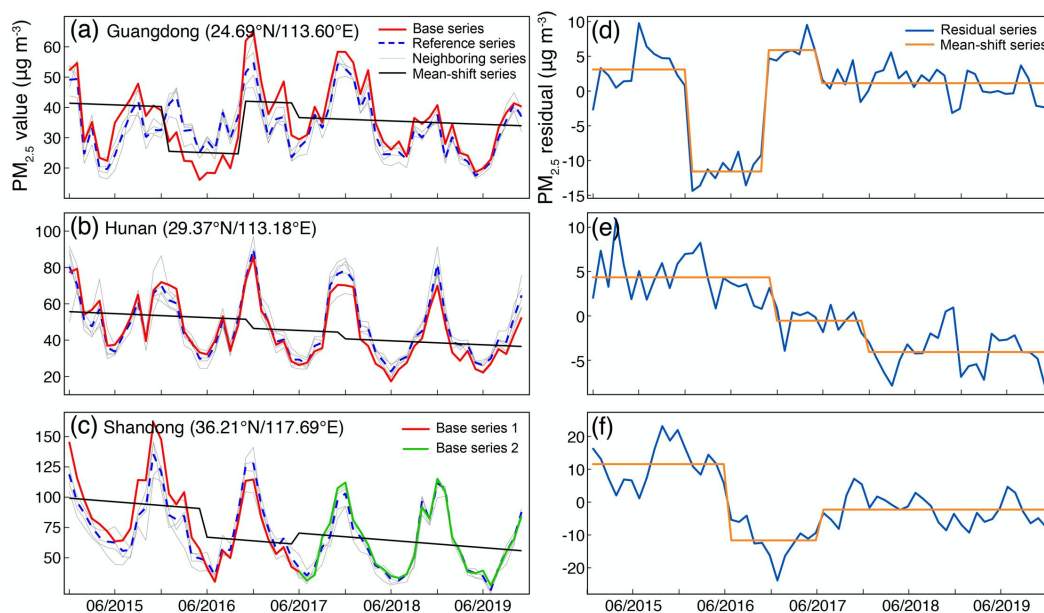


327 **Figure 4.** Temporal variations of the number of change points detected in (a) each specific month from  
328 2015 to 2019 and (b) each month of the year. National mean PM<sub>2.5</sub> concentration in each month of the  
329 year was calculated based on PM<sub>2.5</sub> data measured at our selected 1309 sites during 2015–2019.

330  
331  
332 Due to the lack of essential metadata information, it is a challenge for us to verify each detected  
333 change point through a manual inspection. Rather, the variations in the base and reference series was  
334 explored to identify the possible reasons for the detected discontinuities. Figure 5 presents three typical



335 inhomogeneous  $PM_{2.5}$  time series with different number of change points. The inter-comparisons  
336 between the base and reference series indicate an overall good agreement among them in terms of the  
337 long-term variation tendency. However, obvious drifts were still phenomenal in their residual series,  
338 which were even more evident by referring to their mean-shift series. For example, both the residual  
339 and mean-shift series shown in Figure 5d clearly illustrate a typical discontinuity as there was an  
340 obvious departure of mean  $PM_{2.5}$  concentration level during the period of January to October 2016. In  
341 contrast, the Figures. 5b and 5e present another typical inhomogeneity as statistically significant  
342 decreasing trend was found in the residual series with monthly  $PM_{2.5}$  concentration deviations  
343 decreased from nearly  $5 \mu\text{g m}^{-3}$  to  $-4 \mu\text{g m}^{-3}$  step wise. Such inhomogeneity would undoubtedly result  
344 large bias in the trend estimations over that region. The bottom panel (Figures. 5c and 5f) shows the  
345 change points detected in the merged  $PM_{2.5}$  time series at a pair of relocated sites. It is noteworthy that  
346 the detected discontinuity should be largely ascribed to the inconsistency emerged in the first data  
347 series rather than due to the site relocation.



348

349 **Figure 5.** Temporal variations of three typical inhomogeneous  $PM_{2.5}$  concentration records during  
350 2015–2019. (Top) Significant deviations during a short time period, (middle) long-term chronic drifts  
351 with statistically significant varying trend detected in the residual series, (bottom) discontinuity due to

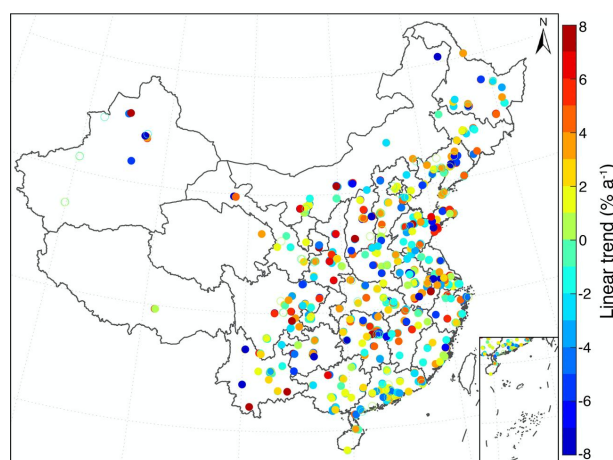


352 site relocation. The left panel compares the base series with the reference and the neighboring series  
353 used to compose the reference while the right panel shows the residual series between the base and  
354 reference series as well as their mean-shift series.

355

356 Figure 6 shows the estimated linear trends for  $PM_{2.5}$  residual series that failed to pass the  
357 homogeneity test. Approximately 89% of the residual series were found exhibiting statistically  
358 significant linear trends, suggesting the vital importance to homogenize such  $PM_{2.5}$  concentration  
359 records as the trend estimations at these stations could be prone to large bias if no essential adjustments  
360 are performed. Further comparisons of the percentage of data gaps between homogeneous and  
361 inhomogeneous records (Figure S2) as well as the spatial distance between the base and the reference  
362 series (Figure S3) indicate that both the frequency of data gaps and spatial distance have no obvious  
363 impact on the change point detection. In other words, the detected change points have no linkage with  
364 neither missing value frequency nor spatial distance between the base and neighboring series,  
365 suggesting a high confidence level of the identified discontinuities in these  $PM_{2.5}$  concentration records.

366

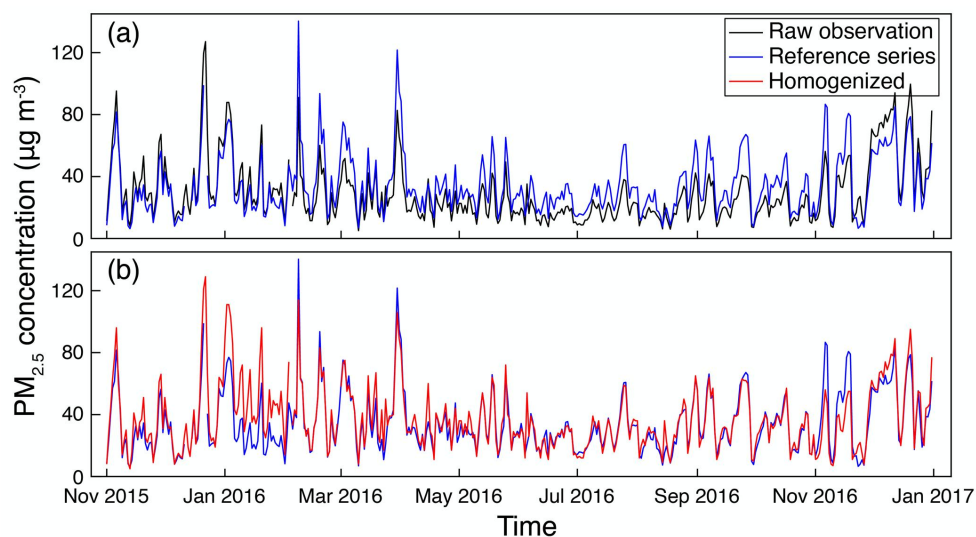


367 **Figure 6.** Trend estimations for the residual  $PM_{2.5}$  concentration data series that failed to pass the  
368 homogeneity test during 2015–2019. The solid circles indicate trends are statistically significant at the  
369 95% confidence level.

370



371           Given the emergence of obvious discontinuities in more than half of the selected long-term PM<sub>2.5</sub>  
372 concentration records, the QM adjustment method was applied to correct the discontinuities detected  
373 in each PM<sub>2.5</sub> concentration record. Figure 7 shows an example of homogenization on PM<sub>2.5</sub>  
374 concentration data series that suffered from evident drifts from its reference (large drifts shown in  
375 Figure 5d). The inter-comparisons of PM<sub>2.5</sub> concentration data between the base and reference series  
376 indicate that the PM<sub>2.5</sub> concentration level was obviously underestimated by the raw observations  
377 compared with the reference, especially during the middle of 2016 (Figure 7a). Such evident drifts  
378 were remarkably diminished after the homogenization (Figure 7b), which shows a good agreement of  
379 the mean PM<sub>2.5</sub> concentration level between the homogenized datum and the reference series.



380  
381 **Figure 7.** Comparison of daily mean PM<sub>2.5</sub> concentration before and after homogenization at one  
382 monitoring site in Guangdong province (24.69°N/113.60°E) from November 2015 to December 2016  
383 (large drifts shown in Figure 5d).

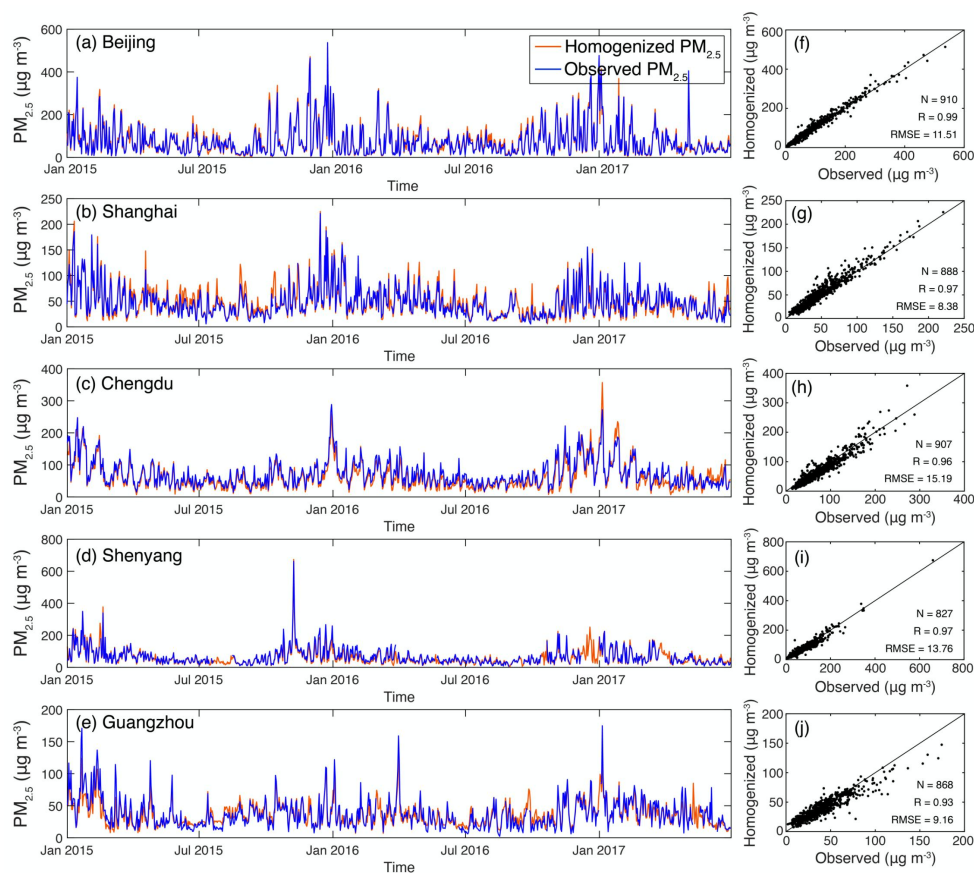
384

#### 385 4.3 Validation with independent dataset

386           In this study, PM<sub>2.5</sub> observations that were collected independently by five consulates of United  
387 States distributed in five major Chinese cities between 2015 and 2017 were used to evaluate the  
388 consistency of the derived PM<sub>2.5</sub> concentration records. Figure 8 shows site-specific comparisons of



389 daily  $PM_{2.5}$  concentration between homogenized and observed data in Beijing, Shanghai, Chengdu,  
390 Shenyang, and Guangzhou, respectively. It is indicative that the homogenized daily  $PM_{2.5}$   
391 concentration data were in good agreement with  $PM_{2.5}$  observations sampled at US consulates, with a  
392 correlation coefficient value of  $>0.95$  and root mean square error of  $<15 \mu g m^{-3}$ . Given the  
393 independent measurement of  $PM_{2.5}$  concentration data at US consulates, we argue that the  
394 homogenized  $PM_{2.5}$  records are accurate enough in characterizing the variability of  $PM_{2.5}$  loadings in  
395 China. It is also noteworthy that the homogenized  $PM_{2.5}$  records are temporally complete whereas  
396 missing values are found in  $PM_{2.5}$  observations sampled at US consulates.



397  
398 **Figure 8.** Comparisons of the homogenized  $PM_{2.5}$  concentration (red) against  $PM_{2.5}$  observations (blue)  
399 measured at five consulates of United States in China from January 2015 to June 2017. (a~e) Temporal  
400 variations of daily  $PM_{2.5}$  concentration and (f~j) the associated scatter plots.



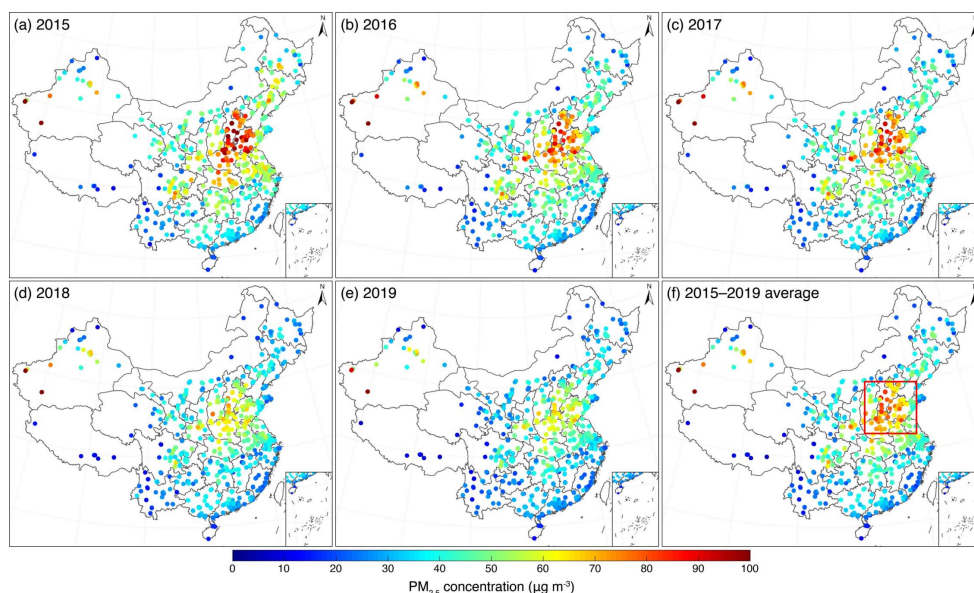
#### 401 4.4 Trend estimations from the homogenized dataset

402 A homogenized data record is essential to trend analysis. Figure 9 presents the annual mean  
403 concentration of PM<sub>2.5</sub> across China from 2015 to 2019. As shown, there is a phenomenal reduction  
404 of PM<sub>2.5</sub> concentration in the past five years, especially in the North China Plain as the annual mean  
405 PM<sub>2.5</sub> concentration decreased from more than 100  $\mu\text{g m}^{-3}$  in 2015 to about 60  $\mu\text{g m}^{-3}$  in 2019. To  
406 evaluate the benefits of data homogenization on PM<sub>2.5</sub> trend estimations, PM<sub>2.5</sub> trends estimated from  
407 both the raw observations and homogenized dataset were compared. Prior to trend analysis, each PM<sub>2.5</sub>  
408 concentration record was standardized in reference to its annual cycle to reduce the impacts of  
409 seasonality and spatial variations. Figure 10 shows a site-specific comparison of PM<sub>2.5</sub> trend  
410 estimations derived from raw observed and homogenized datasets during 2015–2019. In general, trend  
411 estimations from both datasets showed an evident decreasing tendency of PM<sub>2.5</sub> concentration from  
412 2015 to 2019. However, PM<sub>2.5</sub> trends derived from raw observations exhibit obvious inhomogeneity  
413 over space, which is clearly evidenced by the antiphase trend estimations even at adjacent stations,  
414 especially for those with positive trends whereas all adjacent neighbors exhibited negative trends. Such  
415 antiphase trend estimations in a very small region also demonstrate the existence of obvious  
416 inhomogeneity in raw observed *in situ* PM<sub>2.5</sub> concentration dataset.

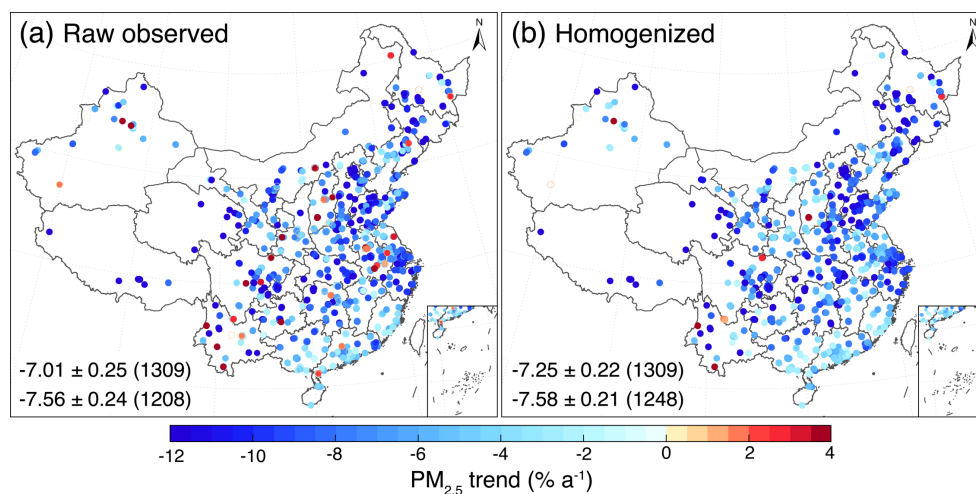
417 After homogenization, the phenomena of antiphase trend estimations over the local region was  
418 substantially diminished, resulting in a spatially much more homogeneous decreasing tendency of  
419 PM<sub>2.5</sub> concentration across China (Figure 10b). This can be also evidenced by the enlargement of  
420 national mean PM<sub>2.5</sub> decreasing trend estimations (increased from 7.01 to 7.25), in particular the  
421 decreased variations in trend values (uncertainty reduced from 0.25 to 0.22) and the increased number  
422 of PM<sub>2.5</sub> records with statistically significant varying trends (1,208 versus 1,248). These results  
423 collectively demonstrate the effectiveness of the QM adjustment method in mitigating such  
424 inhomogeneity, which also highlight the critical importance of data homogenization to account for  
425 discontinuities in this *in situ* PM<sub>2.5</sub> concentration dataset. Overall, our results indicate an obvious  
426 decreasing trend of PM<sub>2.5</sub> concentration in China in the past five years at a mean rate of  $-7.25 \pm 0.22\%$   
427 per year. Compared with other regions of interest (ROIs) such as Pearl River Delta (PRD, refer to



428 Figure S4 for the location),  $PM_{2.5}$  loading over Beijing-Tianjin-Hebei (BTH), Yangtze River Delta  
429 (YRD), Sichuan Basin (SCB), and Central China (CC) decreased even more prominently (Table 1).



430  
431 **Figure 9.** Annual mean  $PM_{2.5}$  concentration derived from the homogenized daily  $PM_{2.5}$  concentration  
432 dataset at 1,309 monitoring stations in China between 2015 and 2019. The North China Plain was  
433 outlined by the red rectangle in panel (f).



434  
435 **Figure 10.** Linear trends for (a) raw observed and (b) homogenized daily  $PM_{2.5}$  concentration data  
436 during 2015–2019. Solid circles indicate trends are statistically significant at the 95% confidence



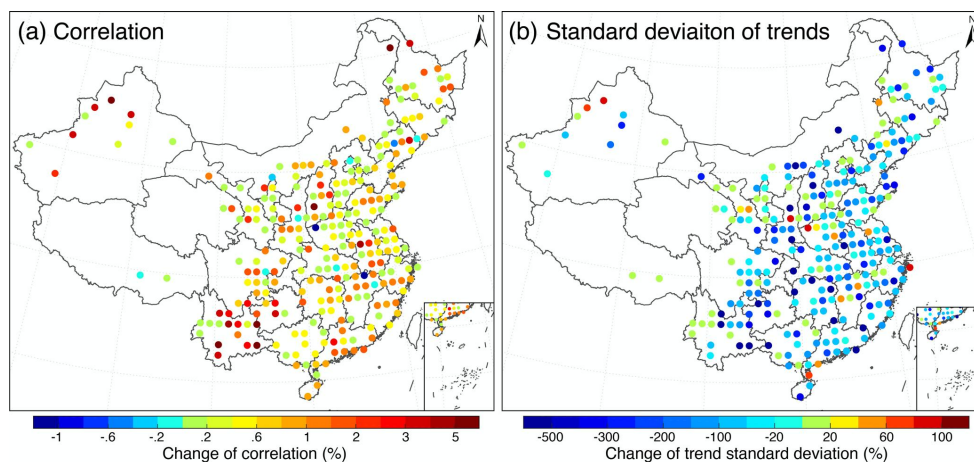
437 interval. Numbers shown in the lower left of each panel indicate the overall trend derived from (top)  
438 all available stations and (bottom) the stations with significant trends at the 95% confidence interval  
439 while the numbers shown in brackets are the corresponding number of data records. Each PM<sub>2.5</sub> time  
440 series were standardized by its mean annual cycle during the study period to account for spatial  
441 variations of PM<sub>2.5</sub>.

442

443 **Table 1.** Regional trend estimations for PM<sub>2.5</sub> concentration over five major ROIs in China during  
444 2015–2019 before and after homogenization. Uncertainty in trend estimations were characterized at  
445 the 95% confidence interval. Locations of these ROIs can be found in Figure S4.

ROI	Raw observation (% a <sup>-1</sup> )	Homogenized record (% a <sup>-1</sup> )
Beijing-Tianjin-Hebei (BTH)	-9.03 ± 0.78	-9.19 ± 0.69
Yangtze River Delta (YRD)	-7.07 ± 0.54	-7.33 ± 0.40
Central China (CC)	-8.47 ± 0.51	-8.58 ± 0.41
Sichuan Basin (SCB)	-7.39 ± 1.02	-7.84 ± 0.89
Pearl River Delta (PRD)	-4.30 ± 0.51	-4.60 ± 0.39

446 To further assess the improvement of the data quality after homogenization, the daily *in situ* PM<sub>2.5</sub>  
447 concentration records at a 1° × 1° grid cell resolution were grouped across China. In each grid cell, the  
448 regional mean correlation coefficient among PM<sub>2.5</sub> concentration time series and standard deviation of  
449 PM<sub>2.5</sub> trends were estimated from the raw observed and homogenized daily PM<sub>2.5</sub> concentration time  
450 series, respectively. Their relative differences were then calculated to show the improvements of data  
451 homogeneity within each grid cell. As shown in Figure 11, the correlation among PM<sub>2.5</sub> concentration  
452 datum was enhanced ubiquitously after homogenization, especially in the southwest of China (e.g.,  
453 Yunnan) where obvious inhomogeneity was observed in the raw PM<sub>2.5</sub> observations (Figure 10a).  
454 Meanwhile, the standard deviation of PM<sub>2.5</sub> trends within each grid cell was also substantially reduced,  
455 even by more than two folds in the magnitude (Figure 11b). These results also demonstrate the critical  
456 need to homogenize the observed PM<sub>2.5</sub> concentration data from a large-scale monitoring network to  
457 reduce temporal inconsistency and spatial inhomogeneity that were not even noticed before.



458

459 **Figure 11.** Spatial distributions of (a) the improvements of mean correlation coefficient among PM<sub>2.5</sub>  
460 concentration records before and after homogenization at a 1° × 1° grid cell resolution across China,  
461 and (b) their corresponding standard deviations of PM<sub>2.5</sub> trends.

462

## 463 5 Data availability

464 The raw observations of *in situ* PM<sub>2.5</sub> concentration data in China used in this study were  
465 retrieved via a web crawler from the National Urban Air Quality Real-time Publishing Platform  
466 (<http://106.37.208.233:20035>) between 2014 and 2019. Given the deployment of many new  
467 monitoring sites in 2014, we decided to generate a coherent PM<sub>2.5</sub> concentration dataset starting from  
468 2015 to include as many records as possible. The homogenized daily *in situ* PM<sub>2.5</sub> concentration dataset  
469 developed in this study is publicly accessible at <https://doi.pangaea.de/10.1594/PANGAEA.917557>  
470 (Bai et al., 2020a).

## 471 6 Conclusions

472 In this study, a homogenized yet temporally complete daily *in situ* PM<sub>2.5</sub> concentration dataset  
473 in China was generated based on the discrete hourly PM<sub>2.5</sub> concentration records that were retrieved  
474 from the National Urban Air Quality Real-time Publishing Platform using a web crawler during the  
475 period of 2015–2019. To create such a coherent dataset, a set of analytic methods were geared up  
476 seamlessly and applied sequentially to the retrieved raw PM<sub>2.5</sub> concentration records, involving quality



477 control, gap filling, data merging, change point detection, and bias correction. This new dataset would  
478 help scientific community better elucidate the temporal and spatial variability of haze pollution in  
479 China in the recent years, which is expected to improve the understanding of underlying causes.

480 The raw  $PM_{2.5}$  concentration records were found to be suffering from phenomenal  
481 inhomogeneity caused by data consistency and temporal coverage as well as the relocation and repeal  
482 of a bunch of monitoring stations. It indicated that more than half of the long-term  $PM_{2.5}$  concentration  
483 records failed to pass the homogeneity test, given the presence of significant change points. Further  
484 investigation confirms that large yet short-term mean shifts and chronic drifts are two primary reasons  
485 for the detected discontinuities.

486 Based on the homogenized dataset, the long-term trends of  $PM_{2.5}$  concentration in China were  
487 estimated. In contrast to the inhomogeneous trend estimations that were derived from raw  $PM_{2.5}$   
488 concentration records, the homogenized dataset yielded a spatially much more homogeneous  
489 decreasing tendency of  $PM_{2.5}$  across China at a mean rate of about  $-7.3\%$  per year. Such an  
490 improvement of homogeneity was also evidenced by the enhanced correlation and reduced standard  
491 deviation of trend estimations between homogenized  $PM_{2.5}$  concentration time series in the  
492 surroundings. These results clearly demonstrate the benefit of data homogenization on the  
493 improvement of the quality of this  $PM_{2.5}$  concentration dataset as evident discontinuities have been  
494 removed after homogenization. Overall, our work clearly reveals the presence of evident  
495 discontinuities in the *in situ*  $PM_{2.5}$  concentration records measured in China, and the homogenization  
496 actions are imperative to take in order to attain a long-term coherent  $PM_{2.5}$  concentration dataset that  
497 can be used to advance  $PM_{2.5}$  pollution related policy making and public health risk assessment.

#### 498 **Author contributions**

499 The study was completed with cooperation between all authors. JG and KB conceived of the idea  
500 behind generating homogenous  $PM_{2.5}$  dataset across China; KB and KL conducted the data analyses  
501 and KB wrote the manuscript; All authors discussed the experimental results and helped reviewing the  
502 manuscript.



503 **Competing interests**

504 The authors declare that they have no conflict of interest.

505

506 **Acknowledgments**

507 This study was financially supported by the National Natural Science Foundation of China (grant  
508 41701413) and the National Key Research and Development Program of China (grant  
509 2017YFC1501401). The authors are grateful to China National Environmental Monitoring Center  
510 (<http://www.cnemc.cn/en/>) and the embassy of United States in China (<http://www.stateair.net/>) for  
511 releasing the sampled air quality data publicly online. We also want to express our sincere thanks to  
512 Dr. Yang Feng in the Expert Team on Climate Change Detection and Indices (ETCCDI)  
513 (<http://etccdi.pacificclimate.org/software.shtml>) for providing the RHtestsV4 software package.

514



515 **References**

- 516 An, Z., Huang, R.J., Zhang, R., Tie, X., Li, G., Cao, J., Zhou, W., Shi, Z., Han, Y., Gu, Z., Ji, Y.,  
517 2019. Severe haze in northern China: A synergy of anthropogenic emissions and atmospheric  
518 processes. *Proc. Natl. Acad. Sci. U. S. A.* 116, 8657–8666.  
519 <https://doi.org/10.1073/pnas.1900125116>
- 520 Anis, A.A., Lloyd, E.H., 1976. The Expected Value of the Adjusted Rescaled Hurst Range of  
521 Independent Normal Summands. *Biometrika* 63, 111–116. <https://doi.org/10.2307/2335090>
- 522 Bai, K., Chang, N.-B., Yu, H., Gao, W., 2016. Statistical bias correction for creating coherent total  
523 ozone record from OMI and OMPS observations. *Remote Sens. Environ.* 182, 150–168.  
524 <https://doi.org/10.1016/j.rse.2016.05.007>
- 525 Bai, K., Chang, N.-B., Zhou, J., Gao, W., Guo, J., 2019a. Diagnosing atmospheric stability effects on  
526 the modeling accuracy of PM<sub>2.5</sub>/AOD relationship in eastern China using radiosonde data.  
527 *Environ. Pollut.* 251, 380–389. <https://doi.org/10.1016/j.envpol.2019.04.104>
- 528 Bai, K., Li, K., Chang, N.-B., Gao, W., 2019b. Advancing the prediction accuracy of satellite-based  
529 PM<sub>2.5</sub> concentration mapping: A perspective of data mining through in situ PM<sub>2.5</sub>  
530 measurements. *Environ. Pollut.* 254, 113047. <https://doi.org/10.1016/j.envpol.2019.113047>
- 531 Bai, K., Li, K., Wu, C., Chang, N.-B., Guo, J., 2020a. A homogenized daily *in situ* PM<sub>2.5</sub>  
532 concentration dataset in China during 2015-2019. PANGAEA,  
533 <https://doi.pangaea.de/10.1594/PANGAEA.917557>
- 534 Bai, K., Li, K., Guo, J., Yang, Y., Chang, N.-B., 2020b. Filling the gaps of in situ hourly PM<sub>2.5</sub>  
535 concentration data with the aid of empirical orthogonal function analysis constrained by diurnal  
536 cycles. *Atmos. Meas. Tech.* 13, 1213–1226. <https://doi.org/10.5194/amt-13-1213-2020>
- 537 Bai, K., Ma, M., Chang, N.-B., Gao, W., 2019c. Spatiotemporal trend analysis for fine particulate  
538 matter concentrations in China using high-resolution satellite-derived and ground-measured  
539 PM<sub>2.5</sub> data. *J. Environ. Manage.* 233, 530–542. <https://doi.org/10.1016/j.jenvman.2018.12.071>
- 540 Cai, W., Li, K., Liao, H., Wang, H., Wu, L., 2017. Weather conditions conducive to Beijing severe  
541 haze more frequent under climate change. *Nat. Clim. Chang.* 7, 257–262.  
542 <https://doi.org/10.1038/nclimate3249>



- 543 Cao, L.-J., Yan, Z.-W., 2012. Progress in research on homogenization of climate Data. *Adv. Clim.*  
544 *Chang. Res.* 3, 59–67. <https://doi.org/10.3724/SP.J.1248.2012.00059>
- 545 Cao, L., Zhao, P., Yan, Z., Jones, P., Zhu, Y., Yu, Y., Tang, G., 2013. Instrumental temperature  
546 series in eastern and central China back to the nineteenth century. *J. Geophys. Res. Atmos.* 118,  
547 8197–8207. <https://doi.org/10.1002/jgrd.50615>
- 548 Ding, A.J., Huang, X., Nie, W., Sun, J.N., Kerminen, V.-M., Petäjä, T., Su, H., Cheng, Y.F., Yang,  
549 X.-Q., Wang, M.H., Chi, X.G., Wang, J.P., Virkkula, A., Guo, W.D., Yuan, J., Wang, S.Y.,  
550 Zhang, R.J., Wu, Y.F., Song, Y., Zhu, T., Zilitinkevich, S., Kulmala, M., Fu, C.B., 2016.  
551 Enhanced haze pollution by black carbon in megacities in China. *Geophys. Res. Lett.* 43, 2873–  
552 2879. <https://doi.org/10.1002/2016GL067745>
- 553 Guo, J.-P., Zhang, X.-Y., Che, H.-Z., Gong, S.-L., An, X., Cao, C.-X., Guang, J., Zhang, H., Wang,  
554 Y.-Q., Zhang, X.-C., Xue, M., Li, X.-W., 2009. Correlation between PM concentrations and  
555 aerosol optical depth in eastern China. *Atmos. Environ.* 43, 5876–5886.  
556 <https://doi.org/10.1016/j.atmosenv.2009.08.026>
- 557 Guo, J., Xia, F., Zhang, Y., Liu, H., Li, J., Lou, M., He, J., Yan, Y., Wang, F., Min, M., Zhai, P.,  
558 2017. Impact of diurnal variability and meteorological factors on the PM<sub>2.5</sub>-AOD relationship:  
559 Implications for PM<sub>2.5</sub> remote sensing. *Environ. Pollut.* 221, 94–104.  
560 <https://doi.org/10.1016/j.envpol.2016.11.043>
- 561 Guo, S., Hu, M., Zamora, M.L., Peng, J., Shang, D., Zheng, J., Du, Z., Wu, Z., Shao, M., Zeng, L.,  
562 Molina, M.J., Zhang, R., 2014. Elucidating severe urban haze formation in China. *Proc. Natl.*  
563 *Acad. Sci.* 111, 17373–17378. <https://doi.org/10.1073/pnas.1419604111>
- 564 He, L., Lin, A., Chen, X., Zhou, H., Zhou, Z., He, P., 2019. Assessment of MERRA-2 Surface PM<sub>2.5</sub>  
565 over the Yangtze River Basin: Ground-based verification, spatiotemporal distribution and  
566 meteorological dependence. *Remote Sens.* 11. <https://doi.org/10.3390/rs11040460>
- 567 He, Q., Huang, B., 2018. Satellite-based mapping of daily high-resolution ground PM<sub>2.5</sub> in China via  
568 space-time regression modeling. *Remote Sens. Environ.* 206, 72–83.  
569 <https://doi.org/10.1016/j.rse.2017.12.018>
- 570 Huang, X., Wang, Z., Ding, A., 2018. Impact of aerosol-PBL interaction on haze pollution: multiyear



- 571        observational evidences in North China. *Geophys. Res. Lett.* 45, 8596–8603.  
572        <https://doi.org/10.1029/2018GL079239>
- 573    Li, Q., Zhang, H., Chen, J.I., Li, W., Liu, X., Jones, P., 2009. A mainland china homogenized  
574        historical temperature dataset of 1951–2004. *Bull. Am. Meteorol. Soc.* 90, 1062–1065.  
575        <https://doi.org/10.1175/2009BAMS2736.1>
- 576    Li, T., Shen, H., Yuan, Q., Zhang, X., Zhang, L., 2017. Estimating ground-level PM<sub>2.5</sub> by fusing  
577        satellite and station observations: A Geo-Intelligent deep learning approach. *Geophys. Res.*  
578        *Lett.* 44, 11,985–11,993. <https://doi.org/10.1002/2017GL075710>
- 579    Li, Z., Guo, J., Ding, A., Liao, H., Liu, J., Sun, Y., Wang, T., Xue, H., Zhang, H., Zhu, B., 2017.  
580        Aerosol and boundary-layer interactions and impact on air quality. *Natl. Sci. Rev.* 4, 810–833.  
581        <https://doi.org/10.1093/nsr/nwx117>
- 582    Lin, C., Li, Y., Lau, A.K.H., Li, C., Fung, J.C.H., 2018. 15-Year PM<sub>2.5</sub> trends in the Pearl River  
583        Delta region and Hong Kong from satellite observation. *Aerosol Air Qual. Res.* 1–8.  
584        <https://doi.org/10.4209/aaqr.2017.11.0437>
- 585    Lin, C.Q., Liu, G., Lau, A.K.H., Li, Y., Li, C.C., Fung, J.C.H., Lao, X.Q., 2018. High-resolution  
586        satellite remote sensing of provincial PM<sub>2.5</sub> trends in China from 2001 to 2015. *Atmos. Environ.*  
587        180, 110–116. <https://doi.org/10.1016/j.atmosenv.2018.02.045>
- 588    Liu, D., Deng, Q., Zhou, Z., Lin, Y., Tao, J., 2018. Variation trends of fine particulate matter  
589        concentration in Wuhan city from 2013 to 2017. *Int. J. Environ. Res. Public Health* 15, 1487.  
590        <https://doi.org/10.3390/ijerph15071487>
- 591    Luan, T., Guo, X., Guo, L., Zhang, T., 2018. Quantifying the relationship between PM<sub>2.5</sub>  
592        concentration, visibility and planetary boundary layer height for long-lasting haze and fog–haze  
593        mixed events in Beijing. *Atmos. Chem. Phys.* 18, 203–225. [https://doi.org/10.5194/acp-18-203-](https://doi.org/10.5194/acp-18-203-2018)  
594        2018
- 595    Ma, Z., Hu, X., Sayer, A.M., Levy, R., Zhang, Q., Xue, Y., Tong, S., Bi, J., Huang, L., Liu, Y., 2015.  
596        Satellite-based spatiotemporal trends in PM<sub>2.5</sub> concentrations: China, 2004–2013. *Environ.*  
597        *Health Perspect.* 124, 184–192. <https://doi.org/10.1289/ehp.1409481>
- 598    Nie, H., Qin, T., Yang, H., Chen, J., He, S., Lv, Z., Shen, Z., 2019. Trend analysis of temperature



- 599 and precipitation extremes during winter wheat growth period in the major winter wheat  
600 planting area of China. *Atmosphere*. 10, 240. <https://doi.org/10.3390/atmos10050240>
- 601 Peterson, T.C., Easterling, D.R., 1994. Creation of homogeneous composite climatological reference  
602 series. *Int. J. Climatol.* 14, 671–679. <https://doi.org/10.1002/joc.3370140606>
- 603 Rodriguez, D., Valari, M., Payan, S., Eymard, L., 2019. On the spatial representativeness of NO<sub>x</sub>  
604 and PM<sub>10</sub> monitoring-sites in Paris, France. *Atmos. Environ.* X 1, 100010.  
605 <https://doi.org/10.1016/j.aeaoa.2019.100010>
- 606 Shen, H., Li, T., Yuan, Q., Zhang, L., 2018. Estimating regional ground-level PM<sub>2.5</sub> directly from  
607 satellite top-of-atmosphere reflectance using deep belief networks. *J. Geophys. Res. Atmos.*  
608 2018JD028759. <https://doi.org/10.1029/2018JD028759>
- 609 Shi, X., Zhao, C., Jiang, J.H., Wang, C., Yang, X., Yung, Y.L., 2018. Spatial representativeness of  
610 PM<sub>2.5</sub> concentrations obtained using observations from network stations. *J. Geophys. Res.*  
611 *Atmos.* 123, 3145–3158. <https://doi.org/10.1002/2017JD027913>
- 612 Wang, G., Zhang, R., Gomez, M.E., Yang, L., Levy Zamora, M., Hu, M., Lin, Y., Peng, J., Guo, S.,  
613 Meng, J., Li, J., Cheng, C., Hu, T., Ren, Y., Wang, Yuesi, Gao, J., Cao, J., An, Z., Zhou, W., Li,  
614 G., Wang, J., Tian, P., Marrero-Ortiz, W., Secretst, J., Du, Z., Zheng, J., Shang, D., Zeng, L.,  
615 Shao, M., Wang, W., Huang, Y., Wang, Yuan, Zhu, Y., Li, Y., Hu, J., Pan, B., Cai, L., Cheng,  
616 Y., Ji, Y., Zhang, F., Rosenfeld, D., Liss, P.S., Duce, R.A., Kolb, C.E., Molina, M.J., 2016.  
617 Persistent sulfate formation from London Fog to Chinese haze. *Proc. Natl. Acad. Sci.* 113,  
618 13630–13635. <https://doi.org/10.1073/pnas.1616540113>
- 619 Wang, X., Wang, K., 2016. Homogenized variability of radiosonde-derived atmospheric boundary  
620 layer height over the global land surface from 1973 to 2014. *J. Clim.* 29, 6893–6908.  
621 <https://doi.org/10.1175/JCLI-D-15-0766.1>
- 622 Wang, X.L., 2008a. Penalized maximal F test for detecting undocumented mean shift without trend  
623 change. *J. Atmos. Ocean. Technol.* 25, 368–384. <https://doi.org/10.1175/2007JTECHA982.1>
- 624 Wang, X.L., 2008b. Accounting for autocorrelation in detecting mean shifts in climate data series  
625 using the Penalized Maximal t or F Test. *J. Appl. Meteorol. Climatol.* 47, 2423–2444.  
626 <https://doi.org/10.1175/2008JAMC1741.1>



- 627 Wang, X.L., Chen, H., Wu, Y., Feng, Y., Pu, Q., 2010a. New Techniques for the Detection and  
628 Adjustment of Shifts in Daily Precipitation Data Series. *J. Appl. Meteorol. Climatol.* 49, 2416–  
629 2436. <https://doi.org/10.1175/2010JAMC2376.1>
- 630 Wang, X.L., Chen, H., Wu, Y., Feng, Y., Pu, Q., 2010b. New techniques for the detection and  
631 adjustment of shifts in daily precipitation data series. *J. Appl. Meteorol. Climatol.* 49, 2416–  
632 2436. <https://doi.org/10.1175/2010JAMC2376.1>
- 633 Wang, X.L., Wen, Q.H., Wu, Y., 2007. Penalized maximal t test for detecting undocumented mean  
634 change in climate data series. *J. Appl. Meteorol. Climatol.* 46, 916–931.  
635 <https://doi.org/10.1175/JAM2504.1>
- 636 Wei, J., Li, Z., Cribb, M., Huang, W., Xue, W., Sun, L., Guo, J., Peng, Y., Li, J., Lyapustin, A., Liu,  
637 L., Wu, H., Song, Y., 2020. Improved 1 km resolution PM<sub>2.5</sub> estimates across China using  
638 enhanced space – time extremely randomized trees. *Atmos. Chem. Phys.* 20, 3273–3289.
- 639 Xin, J., Wang, Y., Wang, L., Tang, G., Sun, Y., Pan, Y., & Ji, D., 2012. Reductions of PM<sub>2.5</sub> in  
640 Beijing-Tianjin-Hebei urban agglomerations during the 2008 Olympic Games. *Adv. Atmos.*  
641 *Sci.*, 29(6), 1330–1342.
- 642 Xu, W., Li, Q., Wang, X.L., Yang, S., Cao, L., Feng, Y., 2013. Homogenization of Chinese daily  
643 surface air temperatures and analysis of trends in the extreme temperature indices. *J. Geophys.*  
644 *Res. Atmos.* 118, 9708–9720. <https://doi.org/10.1002/jgrd.50791>
- 645 Yang, D., Wang, X., Xu, J., Xu, C., Lu, D., Ye, C., Wang, Z., Bai, L., 2018. Quantifying the  
646 influence of natural and socioeconomic factors and their interactive impact on PM<sub>2.5</sub> pollution  
647 in China. *Environ. Pollut.* 241, 475–483. <https://doi.org/10.1016/j.envpol.2018.05.043>
- 648 Yang, Q., Yuan, Q., Yue, L., Li, T., Shen, H., Zhang, L., 2019. The relationships between PM<sub>2.5</sub> and  
649 aerosol optical depth (AOD) in mainland China: About and behind the spatio-temporal  
650 variations. *Environ. Pollut.* 248, 526–535. <https://doi.org/10.1016/j.envpol.2019.02.071>
- 651 You, W., Zang, Z., Zhang, L., Li, Y., Wang, W., 2016. Estimating national-scale ground-level PM<sub>2.5</sub>  
652 concentration in China using geographically weighted regression based on MODIS and MISR  
653 AOD. *Environ. Sci. Pollut. Res.* 23, 8327–8338. <https://doi.org/10.1007/s11356-015-6027-9>
- 654 Zhang, D., Bai, K., Zhou, Y., Shi, R., Ren, H., 2019. Estimating ground-level concentrations of



655 multiple air pollutants and their health impacts in the Huaihe River Basin in China. *Int. J.*  
656 *Environ. Res. Public Health* 16, 579. <https://doi.org/10.3390/ijerph16040579>  
657 Zhang, T., Zhu, Zhongmin, Gong, W., Zhu, Zerun, Sun, K., Wang, L., Huang, Y., Mao, F., Shen, H.,  
658 Li, Z., Xu, K., 2018. Estimation of ultrahigh resolution PM<sub>2.5</sub> concentrations in urban areas  
659 using 160 m Gaofen-1 AOD retrievals. *Remote Sens. Environ.* 216, 91–104.  
660 <https://doi.org/10.1016/j.rse.2018.06.030>  
661 Zhao, P., Jones, P., Cao, L., Yan, Z., Zha, S., Zhu, Y., Yu, Y., Tang, G., 2014. Trend of surface air  
662 temperature in Eastern China and associated large-scale climate variability over the last 100  
663 years. *J. Clim.* 27, 4693–4703. <https://doi.org/10.1175/JCLI-D-13-00397.1>  
664 Zheng, C., Zhao, C., Zhu, Y., Wang, Y., Shi, X., Wu, X., Chen, T., Wu, F., Qiu, Y., 2017. Analysis  
665 of influential factors for the relationship between PM<sub>2.5</sub> and AOD in Beijing. *Atmos. Chem.*  
666 *Phys.* 17, 13473–13489. <https://doi.org/10.5194/acp-17-13473-2017>  
667 Zou, B., Pu, Q., Bilal, M., Weng, Q., Zhai, L., Nichol, J.E., 2016. High-resolution satellite mapping  
668 of fine particulates based on geographically weighted regression. *IEEE Geosci. Remote Sens.*  
669 *Lett.* 13, 495–499. <https://doi.org/10.1109/LGRS.2016.2520480>  
670